Article:

Huang, D., Jia, Z., Hu, Z. et al. (2026) Shared Charging Strategies at the Electric Bus Depot: A Robust Optimization Model. Omega: The International Journal of Management Science. 103634. ISSN: 0305-0483 (In Press)

https://doi.org/10.1016/j.omega.2026.103634

Shared Charging Strategies at the Electric Bus Depot: A Robust Optimization Model

Di Huang[a], Zhou Jia[a], Zhitao Hu[a], Zhiyuan Liu[a,], Ronghui Liu[b,*],*

[a] *School of Transportation, Southeast University, Nanjing, China.*

[b] *Institute for Transport Studies, University of Leeds, Leeds, UK*

***Corresponding author.** Email: zhiyuanl@seu.edu.cn (Zhiyuan Liu), R.Liu@its.leeds.ac.uk (Ronghui Liu)

Abstract

Reservation-based shared charging (R-SC) at bus depots leverages underutilized daytime charging capacity to support private electric vehicle (EV) users while generating additional revenue for bus operators and improving the overall utilization of electric buses (EBs) charging infrastructure. The key challenge, however, is managing the competing charging demands of private EVs without compromising charging reliability and operational needs of EBs. This study introduces a robust optimization modelling framework to schedule same-day EB charging while managing private EV charging demand, accounting for uncertainties in the EB power consumption. Two strategies are proposed to manage the demand of EV charging: a hard charging window with fixed pricing, and a soft charging window with variable, differentiated pricing. Numerical experiments demonstrate that the pricing strategy with the soft charging window better utilizes charging resources, particularly under high EV demand. Prioritizing requests with shorter charging durations leads to a more robust R-SC plan, and time-of-use pricing amplifies the value of the robust model. The finding has practical implications for managing shared charging facilities, and the modelling framework offers a valuable tool for designing resilient and efficient allocation strategies for shared charging.

Keywords: Electric bus; Electric vehicles; Shared charging; Mixed integer programming; Robust optimization

1. Introduction

Electric buses (EBs) are characterized by zero pollutant emissions and low noise emissions, making them an effective solution for transit companies seeking to reduce traffic emissions and operating costs [1–3]. Many countries have committed to the full electrification of urban bus fleets in the near future and are offering subsidies to bus companies to support the transition to full EB fleets.

Despite its benefits, the electrification of urban buses also brings several challenges. First, it requires the construction of extensive charging facilities to ensure reliable bus operations [4–6], at significant costs and financial burden to the bus companies, even with government subsidies. Second, the time-of-use (TOU) electricity pricing incentivizes charging during off-peak nighttime hours, leaving many charging facilities remaining underutilized during the day. At the same time, the growing number of private electric vehicles (EVs) has led to demand for charging infrastructures, outside of their homes and during the day [7–9].

To address the dual challenges faced by both bus companies and private EV owners, shared charging (SC) has emerged as an effective solution [10]. The concept of SC involves bus companies making their charging infrastructure at bus depots available to private EVs. In return, bus companies collect service fees from private EV owners, creating an additional revenue stream. For private EV owners, it introduces an additional charging option, helping to alleviate range anxiety [11]. From a societal perspective, SC enhances overall resource efficiency and incentivizes bus companies to expand their EB services, thereby contributing to the advancement of transportation electrification. SC has been widely implemented in China, with 70% of bus depots in Guangzhou offering public charging services as of 2023 [12].

Existing research on SC primarily focuses on its impact on overall system efficiency [13,14]. At the operational level, most studies concentrate on scheduling and charging plans for EBs, often simplifying the charging demand of EVs [15,16]. However, operational-level strategies for allocating charging resources to EVs remain unexplored, despite being critical to the economic feasibility of SC from the bus company's perspective. This highlights the need for a systematic investigation into operational-level SC strategies and modeling frameworks.

This study investigates a reservation-based shared charging (R-SC) strategy at the operational level. Within this framework, the bus company gathers private EV charging requests and EB service schedule (on service route and vehicle-to-trip assignment), and plans for an optimal allocation of charging resources for EBs and private EVs for the following day. The integrated optimization aims at maximizing the bus company's benefits while ensuring the stable operation of EBs. To ensure the reliability of EB operations, a robust optimization model considering uncertainty in EB energy consumption is developed. Two distinct SC pricing strategies are proposed and evaluated on their impact on depot operations: (1) providing charging services only within the originally requested time window; (2) extending the charging window beyond the original request, offering the original price within the requested window and a discounted price in the extended period. The effectiveness of the R-SC plan is tested using a real-world case study at Lianyungang Station, offering valuable managerial insights.

1.1 Literature review

Due to limited battery capacity, the driving range of EBs is restricted. On routes with long travel distances, EBs must recharge during operation to complete all scheduled trips. Consequently, charging schedule is a key aspect of EB operations [17]. Abdelwahed et al. [18] propose two models, a discrete-time optimization and a discrete-event optimization, to address the EB opportunity charging problem. Liu et al. [19] develop a mixed-integer programming model for the resource-constrained EB charging problem and solve it using a column-generation-based algorithm. Whitaker et al. [20] introduce a network-flow-based integer programming model to optimize EB charging under resource constraints. Zeng et al. [21] incorporate battery degradation into the charging decision-making. Bao et al. [22] investigate the optimal charging strategy for EBs across multiple charging stations. Wu et al. [23,24] study the charging and scheduling problem of EBs in a multi-depot setting with consideration of power grid characteristics, and further extend their work to online scenarios. Yang et al. [25] integrate electric bus scheduling with battery charging in swapping mode.

EB energy consumption is highly uncertain due to factors such as weather conditions, traffic fluctuations, and varying passenger demand. To address this variability, uncertainty optimization methods can be employed to model energy consumption fluctuations, ensuring more reliable EB operation planning. An [26] considers the uncertainty in EB charging demand and develops a stochastic integer programming model for EB infrastructure planning. Zeng et al. [27] propose a robust optimization model for the EB en-route charging scheduling, accounting for energy consumption uncertainty. Zhou et al. [28] formulate a robust optimization framework that integrates EB charger deployment and charging scheduling. Huang et al. [29] investigate a charging scheduling problem that combines plug-in charging and battery swapping, constructing a robust optimization model that incorporates the uncertainty in EB state-of-charge levels.

In recent years, shared charging at EB depots has attracted growing attention. This approach enhances the utilization of idle charging resources at bus depots while helping to mitigate the shortage of public charging infrastructure. Ye et al. [13] integrate shared charging with vehicle-to-grid technology and assess its impact on reducing carbon emissions. Zhang et al. [14] construct a tripartite game model to explore the effects of government incentive and penalty mechanisms on different stakeholders. Ji et al. [15] propose a model integrating the EB scheduling problem with shared charging, assuming that the arrival of EVs follows a Poisson distribution. Liu et al. [16] introduce a new business model that integrates shared charging with solar photovoltaic technology and employs queuing theory to characterize EV charging demand. Wang et al. [30] develop a real-time shared charging scheduling system to enhance the overall charging efficiency of a heterogeneous electric vehicle fleet. Jia et al. [31] focus on determining the optimal number of chargers open to EVs in each period and formulate a two-stage stochastic optimization model to maximize bus company revenue.

1.2 Aim and contributions

This study addresses the R-SC problem at a single bus depot and proposes an integrated optimization framework that jointly optimizes the charging schedules for EBs and EVs, with the objective to minimize the bus company's operational costs while ensuring the stable operation of their EB services. To further guarantee the stable operation of EBs, a robust optimization model is introduced, which takes into account the uncertainty in EB energy consumption during operation.

This study contributes to the state-of-the-art in SC in the following ways. First, it introduces an R-SC problem that simultaneously determines the charging schedules for both EBs and EVs, effectively optimizing the utilization of limited charging resources. Second, the R-SC is formulated in an optimization model that maximizes the revenue of the bus company. To ensure the stable operation of EBs, a robust optimization model is proposed that accounts for the uncertainty in the energy consumption of EBs during operation. Third, the study proposes two different pricing strategies and evaluates their impacts on depot operations, providing insights on the practical implementation of SC schemes.

The remainder of this study is structured as follows. Section 2 provides a formal problem statement of the R-SC and formulates it as a deterministic mixed integer linear programming (MILP) model. An extension to account for uncertainties in EBs' energy consumption is introduced, and a robust model is proposed in Section 3. Section 4 analyzes the results of the numerical experiments by real-world data in Lianyungang. Section 5 presents our conclusions.

2. Problem Statement and a Deterministic Model of Shared Charging

2.1 Notations

For ease of presentation, notations in this section are introduced in Table 1.

Table 1 List of notations.

Notation	Description
Sets	
I	The set of requests from private EVs, $i \in I$.
J	The set of EBs, $j \in J$.
N_j^{cw}	The set of indices of charging windows for EB j, $n \in N_j^{cw}$.
N_j^{ow}	The set of indices of operating windows for EB j, $n \in N_j^{ow}$.
T	The set of time slots, $t \in T$.
T_i	The set of time slots in charging time window for private EV i, $t \in T_i$.
$T_{j,n}^{cw}$	The set of time slots in the n-th charging windows for EB j, $t \in T_{j,n}^{cw}$.
$T_{j,n}^{ow}$	The set of time slots in the n-th operating windows for EB j, $t \in T_{j,n}^{ow}$.

Parameters

c^t	The unit electricity cost price for charging pile within time slot t.
K	The available number of charging piles.
p_i^t	The fee for private EV i within time slot t charged by EB operators.
$p^{regular}$	The regular service fee for unit electricity.
p^{lower}	The special service fee for unit electricity which is lower than the regular service fee.
q	The amount of electricity charged during one time slot.
Δ	The offset used to construct the soft charging window.
s_i	The index of start time slot of acceptable time window for private EV i.
e_i	The index of end time slot of acceptable time window for private EV i.
α_i	The requested number of time slots for private EV i to be charged.
β_j	The minimum number of time slots for EB j to be charged.
δ_j	The battery capacity of EB j.
$\tau_j^{\min}$	The minimum allowed State of Charge (SoC) for EB j.
$\tau_j^{\max}$	The maximum allowed SoC for EB j.
$s_{j,n}^{cw}$	The start time of charging time window for EB j in charging time window $T_{j,n}^{cw}$.
$e_{j,n}^{cw}$	The end time of charging time window for EB j in charging time window $T_{j,n}^{cw}$.
$s_{j,n}^{ow}$	The start time of charging time window for EB j in operating time window $T_{j,n}^{ow}$.
$e_{j,n}^{ow}$	The end time of charging time window for EB j in operating time window $T_{j,n}^{ow}$.
$\pi_{j,n}^{ow}$	The amount of electricity consumed by the EB j within operating time window $T_{j,n}^{ow}$.

Decision variables

x_j^t	A binary variable for the decision on the charging schedule of EB, i.e., $x_j^t = 1$ if EB j is charged in time slot t; $x_j^t = 0$, otherwise.

y_i^t	A binary variable for the decision on the charging schedule of private EV, i.e., $y_i^t = 1$ if private EV i is charged in time slot t; $y_i^t = 0$, otherwise.
Auxiliary variables	
b_j^t	A continuous variable representing the battery level of the EB j at the start of time slot t.
z_j^t	A binary variable indicating the start of the charging session for EBs, i.e., $z_j^t = 1$ if EB j starts charging in time slot t; $z_i^t = 0$,otherwise.
$W_j(n)$	A continuous variable representing the cumulative charging amount of EB j over its first n charging windows.

2.2 Problem description

This study focuses on the SC plan of a single depot, equipped with a fixed number of charging piles. We consider that the SC operates during the day, and the planning horizon is divided into discrete time slots (illustrated as boxes in Fig. 1). To facilitate understanding, Fig. 1 presents an illustrative example of the integrated charging plan using a simplified setting with one EB, two EVs, and a single charging pile.

Firstly, SC plan must ensure the stable operation of EBs. The planning horizon of EBs can be divided into two sets: the operating windows, during which EBs are out on service runs (shown as yellow boxes in Fig. 1a), and the charging windows, when they return to the depot and are available for recharging (shown as green boxes in Fig. 1a). An EB typically has multiple charging windows throughout the planning horizon, but it is not necessarily charged in every window. Charging is performed as needed to keep the SoC within a safe range.

Secondly, private EV requests consist of a charging window and the desired charging duration. For example, in Fig. 1b, EV1 submits a request with a 4-slot time window and expects to receive 3 slots of charging service.

Finally, based on the charging demands of both EBs and private EVs, the bus company allocates charging resources to maximize overall profit. Due to limited capacity, some EV charging requests may be rejected. As illustrated in Fig. 1c, which reflects the requests in Figs.

1a and 1b, EB1 receives sufficient charging to maintain reliable operation, EV1 is successfully served, while EV2 is rejected due to insufficient charging availability.

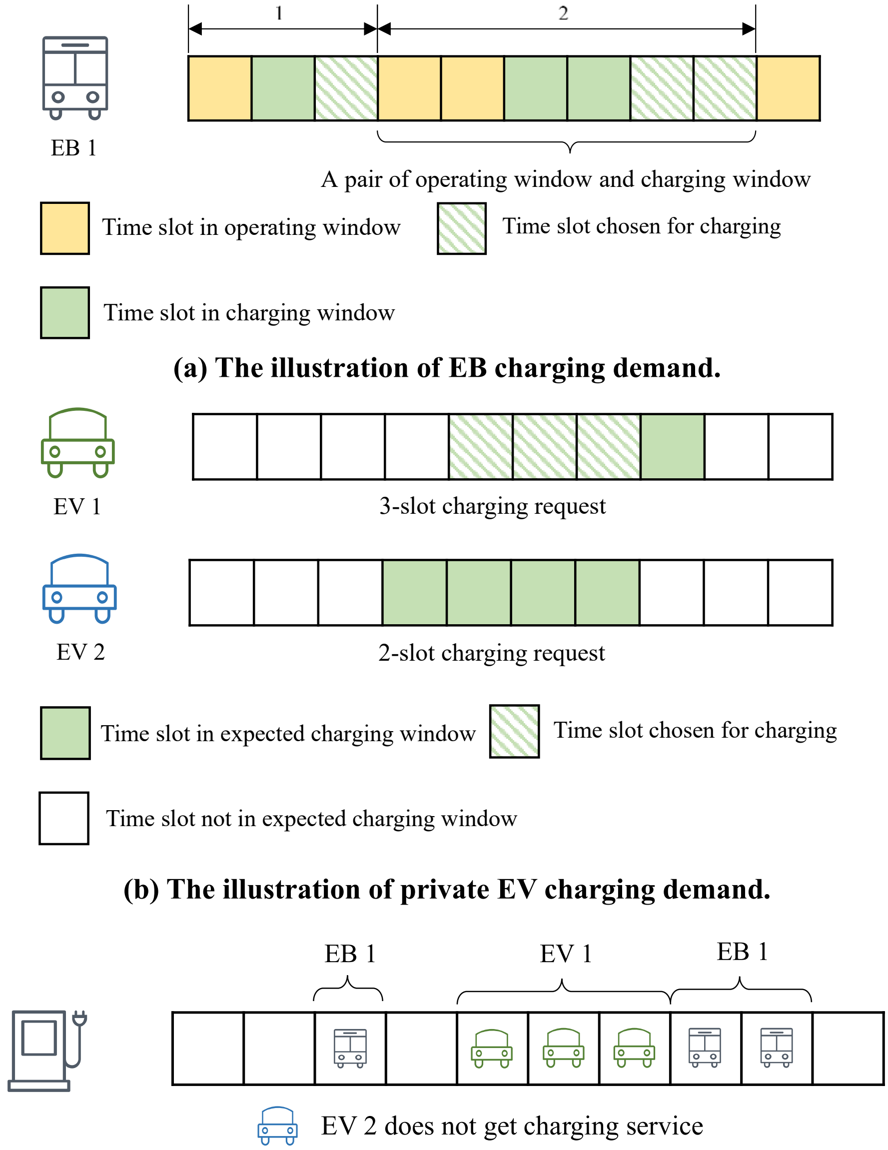

(a) The illustration of EB charging demand.

(b) The illustration of private EV charging demand.

(c) The illustration of the shared charging plan.

Figure 1 Illustration of shared charging plan.

Without loss of generality, the following assumptions are made: (1) The number of charging piles at a single bus depot is finite and sufficient to ensure reliable EB operations; (2) EB fleet undergoes centralized recharging overnight and will start the day with full charge; (3) There is a minimum charging period for both EBs and EVs; (4) EB may need multiple re-charges during planning horizon; (5) on-the-day EV charging requests are not considered.

2.3 Model formulation

This study considers an R-SC plan for a single bus depot. The planning horizon of the depot is divided into several time slots of equal duration. Let T denote the set of time slots. The time slots for EB $j \in J$ is grouped into operating windows and charging windows. Let N_j^{ow} and N_j^{cw} denote the index sets of operating windows and charging windows of EB j. If $n \in N_j^{ow}$, it refers to the n-th operating window of EB j; If $n \in N_j^{cw}$, it refers to the n-th charging window of EB j. Let $T_{j,n}^{cw} \subseteq T$ denote the set of time slots in the n-th charging window for EB j, with a start time $s_{j,n}^{cw}$ and end time $e_{j,n}^{cw}$. Let $T_{j,n}^{ow} \subseteq T$ denote the set of time slot in n-th operating window for EB j, with start time $s_{j,n}^{ow}$ and end time $e_{j,n}^{ow}$.

The time slots for each EB are structured as shown in Figure 2. Operating and charging windows alternate throughout the day. By design, the end time of the n-th operating window coincides with the start time of the n-th charging window, and the end time of the n-th charging window coincides with the start time of the $n+1$-th operating window, that is, $e_{j,n}^{ow} = s_{j,n}^{cw}$, $\forall j \in J, n \in N_j^{ow} \cap N_j^{cw}$, and $e_{j,n}^{cw} = s_{j,n+1}^{ow}$, $\forall j \in J, n \in N_j^{cw}$. The planning horizon of EB always starts and ends with an operating window.

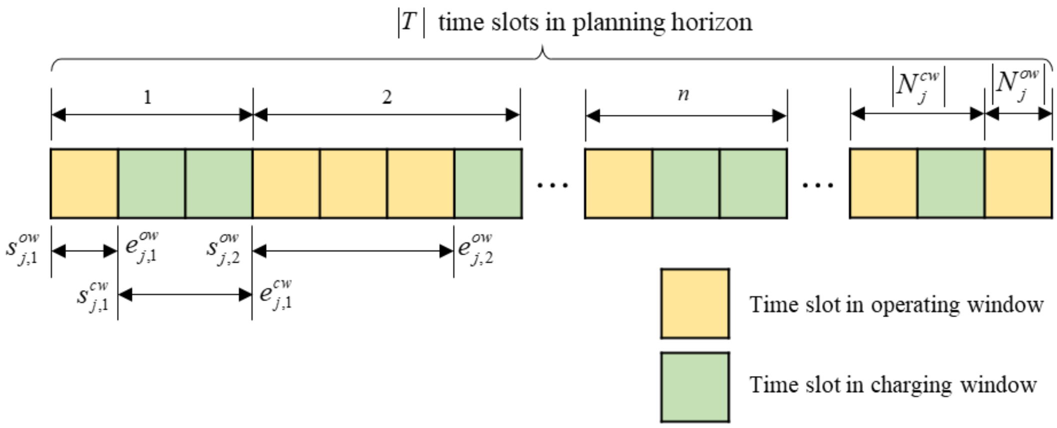

Figure 2 Illustration of alternating operating and charging windows for EBs.

Remark 1. This study focuses exclusively on daytime operations at the bus depot. The first time window for each EB is always an operating window, as all EBs are assumed to be fully charged at the beginning of the planning horizon and therefore do not require immediate charging. Similarly, the last time window is also an operating window. If the last window were a charging window, no actual charging would occur during this period, since the EB would have already completed all scheduled trips and would no longer consume energy. This assumption is practical, as EBs can be recharged overnight using slow chargers at lower electricity rates, thereby reducing overall charging costs.

The amount of electricity consumed by EB j within operating time window $T_{j,n}^{ow}$ is denoted by $\pi_{j,n}^{ow}$. The battery capacity of EB $j \in J$ is denoted by δ_j. To ensure stable operation, EB j must maintain its battery level above τ_j during operation. Considering real-world charging behaviors, the number of time slots in a single charging session for an EB j cannot be lower than β_j.

The set of requests from private EVs is denoted by I. Each request $i \in I$ consists of two components: the charging time window and the requested number of time slots for charging α_i. The set of time slots in the charging time window for private EV is denoted by T_i, with the start time s_i and end time e_i. It is assumed that the duration of the time window $e_i - s_i$ is always longer than α_i.

The bus depot is equipped with a fixed number of charging piles, which are sufficient to support stable EB operations. A charging pile can deliver a fixed quantity of electricity q within one time slot. The cost of electricity supplied by a charging pile in time slot t, denoted as c^t, is regulated by the government and varies with TOU rates. The service fee for unit electricity from the charging pile in time slot t is p^t, which is determined by the EB operator.

2.3.1 EB charging model

EBs undergo multiple charging and discharging cycles during operation. To facilitate the construction of the subsequent R-SC model, it is essential to first develop a model that captures the changes in EB battery levels throughout the operation. The energy variation process includes three key steps: battery initialization, charging, and discharging. A binary variable x_j^t is introduced to indicate whether the EB j is charging during time slot t, while a continuous variable b_j^t is used to track the battery level of EB j at the start of time slot t. Eqs. (1)–(4) describe the EB charging process in detail.

Eq. (1) defines the domains of decision variables of EB charging.

$$x_j^t \in \{0,1\} \quad \forall j \in J, t \in T \tag{1}$$

Eq. (2) initializes the battery level of all EBs at the start of the day.

$$b_j^s = \tau_j^{\max} \delta_j \quad \forall j \in J, s = s_{j,1}^{ow} \tag{2}$$

Eq. (3) establishes the relationship between the battery levels at the start and end times of each operating window for an EB. During these periods, EBs are providing service on the road, which results in energy consumption. Since charging is not permitted within operating windows, the model focuses solely on the battery levels at the beginning and end of each window, without modeling the battery levels at intermediate time points.

$$b_j^e = b_j^s - \pi_{j,n}^{ow} \quad \forall j \in J, n \in N_j^{ow}, s = s_{j,n}^{ow}, e = e_{j,n}^{ow} \tag{3}$$

Eq. (4) regulates the alteration in EB battery levels during charging windows. If $x_j^t = 1$, it indicates that the EB is being charged during the time slot t, and the battery level will accordingly increase.

$$b_j^{t+1} = b_j^t + q x_j^t \quad \forall j \in J, n \in N_j^{cw}, t \in T_{j,n}^{cw} \tag{4}$$

Based on Eqs. (1)–(4) and the defined relationships between charging windows and operating windows in Section 3.2, the proposed model provides a complete representation of EB operations. It captures both the scheduling structure and the battery levels at all critical time points during operation.

2.3.2 Reservation-based shared charging model

The R-SC model is formulated by integrating three main components: EB charging constraints, depot resource constraints, and service strategies. The details are presented as follows.

(1) EB charging constraints

Eq. (5) prohibits EBs from charging during the operating windows.

$$x_j^t=0 \quad \forall j \in J, n \in N_j^{ow}, t \in T_{j,n}^{ow} \tag{5}$$

Eqs. (6)–(7) ensure that each EB charging session meets a minimum duration requirement. Within the specified charging time window, an EB can choose whether to charge, but if charging is initiated, the charging session must last for β time slots. $x_j^t - x_j^{t-1} = 1$ denotes the start of charging session at the time slot t.

$$z_j^t = x_j^t - x_j^{t-1} \quad \forall j \in J, n \in N_j^{ow}, t \in T_{j,n}^{ow} \tag{6}$$

$$x_j^{t+u} \geq z_j^t \quad \forall j \in J, n \in N_j^{cw}, t \in \left[s_{j,n}^{cw}, e_{j,n}^{cw} - \beta_j\right], u \in \left[1, \beta_j - 1\right] \tag{7}$$

Eq. (8) complements the minimum EB charging duration by eliminating infeasible charging plans within the last β_j time slots. Figure 3 illustrates an example of a violation of the minimum charging duration constraint where $\beta_j = 4$. In this case, the EB only charges during the last two time slots within the charging window. Although this charging plan satisfies Eq. (8), the actual charging duration falls short of the required minimum.

$$z_j^t = 0 \quad \forall j \in J, n \in N_j^{cw}, t \in \left[e_{j,n}^{cw} - \beta_j, e_{j,n}^{cw} - 1\right] \tag{8}$$

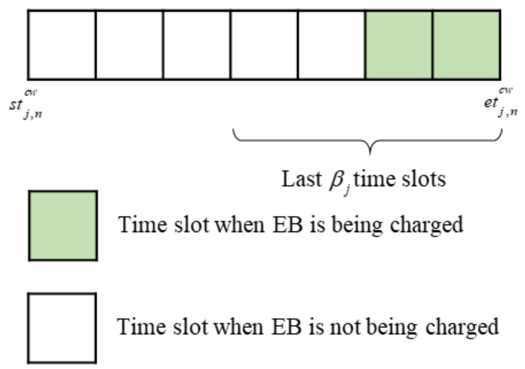

Figure 3 Illustration of unreasonable EB charging instances.

Eq. (9) ensures that the EB's battery level remains within a healthy operating range throughout its operation.

$$\tau_j^{\min}\delta_j \le b_j^t \le \tau_j^{\max}\delta_j \quad \forall j \in J, t \in T \tag{9}$$

(2) Depot resource constraints

$$\sum_{i\in I} y_i^t + \sum_{j\in J} x_j^t \le K \quad \forall t \in T \tag{10}$$

Eq. (10) represents the capacity constraint of the charging piles. Within a specified time slot, the number of charging piles available at the depot is limited.

(3) Service strategies

Two pricing strategies, **[M1]** and **[M2]**, are proposed in this study. The primary differences between the **[M1]** and **[M2]** models lie in the settings of service fee p_i^t and the allowed charging time range. A parameter Δ is introduced to control the allowed charging time range. To provide a unified formulation, a general model **[GM]** is first presented, from which **[M1]** and **[M2]** can be obtained by adjusting p_i^t and Δ accordingly.

[GM]

$$\min \sum_{j\in J}\sum_{t\in T} qc^t x_j^t + \sum_{i\in I}\sum_{t\in T} qc^t y_i^t - \sum_{i\in I}\sum_{t\in T} p_i^t y_i^t \tag{11}$$

Subject to Eqs. (1)–(10) and

$$y_i^{t+u} \ge y_i^t \quad \forall i \in I, t = s_i - \Delta, u \in [1, \alpha_i - 1] \tag{12}$$

$$y_i^{t+u} \ge y_i^t - y_i^{t-1} \quad \forall i \in I, t \in [s_i - \Delta + 1, |T| - \alpha_i], u \in [1, \alpha_i - 1] \tag{13}$$

$$\sum_{t=s_i-\Delta}^{e_i+\Delta} y_i^t \le \alpha_i \quad \forall i \in I \tag{14}$$

$$y_i^t = 0 \quad \forall i \in I, t \in T \setminus \{t \in T \mid s_i - \Delta \le t \le e_i + \Delta\} \tag{15}$$

$$y_i^t \in \{0,1\} \quad \forall i \in I, t \in T \tag{16}$$

Eq. (11) denotes the objective for the R-SC model. The first part and second part of the objective function denote the charging cost for EBs and EVs, respectively. The third part is the fee charged by the EB operator for providing charging services to the EVs. The pricing of the fee can vary across different periods for different EVs, which will be discussed in detail in the part on service strategies.

Eqs. (12)–(16) are the constraints related to the charging service for private EVs. For EV charging requests, the operator can decide whether to provide the service. If the service is provided, it must be completed in a single, continuous charging session. Eq. (12)–(13) mandate that a continuous charging duration must be maintained if EV i is served, where $y_i^t - y_i^{t-1} = 1$ denotes the initiation of charging at time slot t. Eq. (14) ensures that the cumulative charging duration of EV i does not exceed its required charging time α_i. Eq. (15) stipulates that charging can only be provided in private EV's charging window. Eq. (16) defines the domains of decision variables related to EV charging.

In the **[M1]** model, $\Delta = 0$ means that only the charging resources within the charging window are allocated to EVs. The pricing within this window remains constant, regardless of time.

In contrast, the **[M2]** model adopts a more flexible design in service windows. Specifically, $\Delta > 0$ means that **[M2]** extends the hard charging window specified by EV users by expanding it forward and backward by Δ time slots, creating a wider soft charging window. Charging resources within the soft charging window $\{t \in T \mid s_i - \Delta \le t \le e_i + \Delta\}$ can be allocated to EVs.

Moreover, the **[M2]** model adopts a flexible pricing strategy, as is shown in Eq. (17). Within the charging window, a regular price $p^{regular}$ is applied; outside the hard charging window, a lower price p^{lower} is charged. This pricing mechanism promotes more efficient utilization of charging resources.

$$p_i^t = \begin{cases} p^{regular} + qc^t & \text{if } t \in [s_i, e_i] \\ p^{lower} + qc^t & \text{if } t \in [s_i - \Delta, s_i] \cup [e_i, e_i + \Delta] \end{cases} \quad \forall i \in I \tag{17}$$

3. A robust model of R-SC

The energy consumption of EBs during operation is subject to uncertainty due to factors such as vehicle performance, temperature, and road conditions. To ensure the stable operation of the EB fleet, it is essential to account for these uncertainties when developing an R-SC plan. When designing the R-SC plan, priority should be given to ensuring the stable operation of bus services. Therefore, the energy level of the EB must always remain within the acceptable range during operation under all circumstances. To achieve this goal, a robust model is formulated based on the deterministic model presented in Section 2. Robust optimization addresses parameter uncertainty using an uncertainty set, ensuring that the solution satisfies the model's constraints under any realization of the uncertainty parameters within this set. In this study, the energy consumption of EBs within the operating window is treated as an uncertain parameter.

3.1 Uncertainty set

The random parameter $\tilde{\pi}^{ow}_{j,n}$ is introduced to represent the energy consumption of EB j during the n-th operating window, which can be described by the following equation:

$$\tilde{\pi}^{ow}_{j,n} = \overline{\pi}^{ow}_{j,n} + \eta_{j,n}\hat{\pi}^{ow}_{j,n} \quad \forall j \in J, n \in N^{ow}_{j} \tag{18}$$

where $\eta_{j,n} \in [-1,1]$ denotes the uncertainty parameter, $\overline{\pi}^{ow}_{j,n}$ represents the mean energy consumption of EB j during the n-th operating window, and $\hat{\pi}^{ow}_{j,n}$ denotes the standard deviation of the energy consumption during the n-th operating window. Similar to (Zeng et al., 2024), the standard deviation is set as $\hat{\pi}^{ow}_{j,n} = \gamma\overline{\pi}^{ow}_{j,n}$ and $0 \le \gamma \le 1$.

The budgeted uncertainty set [32] is adopted to describe the uncertainty of the energy consumption of EBs. The conventional box uncertainty set is overly conservative, whereas the budgeted uncertainty set allows for the control of decision-making conservatism through parameters. Furthermore, the budgeted uncertainty set has been widely applied in integer programming problems [33–35]. The uncertainty sets for energy consumption are given below.

$$\phi^{n}_{j} = \left\{ \boldsymbol{\eta}^{\mathbf{n}}_{\mathbf{j}} : \left|\boldsymbol{\eta}^{\mathbf{n}}_{\mathbf{j}}\right| \le 1,\ \sum_{n'=1}^{n} \left|\eta^{n}_{j,n'}\right| \le \Gamma^{n}_{j} \right\} \quad \forall j \in J, n \in N^{ow}_{j} \tag{19}$$

where ϕ^{n}_{j} denotes the uncertainty set for the energy consumption of EB j during the n-th operating window, $\boldsymbol{\eta}^{\mathbf{n}}_{\mathbf{j}} = \left[\eta^{n}_{j,1}, \eta^{n}_{j,2}, \eta^{n}_{j,3}, \ldots, \eta^{n}_{j,n'}, \ldots, \eta^{n}_{j,n}\right]$ is the vector of all the uncertainty parameters in the row, Γ_j^n is the parameter that controls the conservatism of the decision.

3.2 Robust counterpart

By replacing the relevant parameters in the deterministic model with random parameters, the original integer programming problem is transformed into a semi-infinite programming problem. Solving semi-infinite programming problems directly is challenging. It is necessary to reformulate the problem into a tractable formulation that a commercial solver can solve efficiently. The result of the reformulation is commonly referred to as the robust counterpart [36].

To facilitate the derivation of the robust counterpart, certain constraints in the original model (Eqs. (2)–(4) and Eq. (9)) are reformulated into a structure suitable for robust optimization. The purpose of this step is to shift the uncertain parameters from equality constraints into inequality constraints, since robust counterpart derivations are applicable only when uncertain parameters appear in inequality constraints.

Consider the EB battery bounds in Eq. (9). It can be observed that the maximum SoC must occur at the end of a charging window, while the minimum SoC must occur at the end of an operating window. Therefore, it is sufficient to ensure that the SoC at the end of each operating window is no less than the lower bound, and that the SoC at the end of each charging window does not exceed the upper bound. For notational simplicity, let $W_j(n) = \sum_{n'=1}^{n} \sum_{t=s_{j,n'}^{cw}}^{e_{j,n'}^{cw}-1} qx_j^t$ denote the cumulative charging amount of EB j over its first n charging windows.

We first derive the constraint ensuring that the SoC at the end of the n-th charging window is no less than the lower bound. In Eq. (20), the first term represents the EB's initial battery level at departure, the second term denotes the cumulative amount of energy charged by the end of the n-th charging window, and the third term accounts for the cumulative energy consumption by the same point.

$$b_j^e = \tau_j^{\max}\delta_j + W_j(n) - \sum_{n'=1}^{n} \tilde{\pi}_{j,n'}^{ow} \le \tau_j^{\max}\delta_j \quad \forall j \in J, n \in N_j^{cw} \tag{20}$$

By simplifying Eq. (20), we obtain Eq. (21):

$$\sum_{n'=1}^{n} \tilde{\pi}_{j,n'}^{ow} \geq W_j\left(n\right) \quad \forall j \in J, n \in N_j^{cw} \tag{21}$$

Next, the robust counterpart of Eq. (21) is derived. Since Eq. (21) imposes a lower-bound inequality, it suffices to verify the condition under the minimum value of its left-hand side. If the inequality holds in this case, it will hold for all realizations within the uncertainty set. To ensure that Eq. (21) holds for any value of $\eta_{j,n}$, $\eta_{j,n}$ is treated as a decision variable, and the left-hand side of Eq. (21) is set as the objective function. This leads to the construction of the auxiliary minimization problem **[P1]**.

[P1]

$$\min \ \sum_{n'=1}^{n} \overline{\pi}_{j,n'}^{ow} + \sum_{n'=1}^{n} \hat{\pi}_{j,n'}^{ow} \eta_{j,n'}^{n} \tag{22}$$

s.t.

$$\left|\eta_{j,n'}^{n}\right| \leq 1 \ \ \forall n' \in \left[1, n\right] \tag{23}$$

$$\sum_{n'=1}^{n} \left|\eta_{j,n'}^{n}\right| \leq \Gamma_j^n \tag{24}$$

Since $\hat{\pi}_{j,n'}^{ow} > 0$, in order to minimize the objective function, $\eta_{j,n'}^{n}$ must necessarily take negative values. This leads to the following result:

[P1–A]

$$\min \ \sum_{n'=1}^{n} \overline{\pi}_{j,n'}^{ow} + \sum_{n'=1}^{n} \hat{\pi}_{j,n'}^{ow} \eta_{j,n'}^{n} \tag{25}$$

s.t.

$$-1 \leq \eta_{j,n'}^{n} \leq 0 \ \ \forall n' \in \left[1, n\right] \tag{26}$$

$$-\sum_{n'=1}^{n} \eta_{j,n'}^{n} \leq \Gamma_j^n \tag{27}$$

The dual variables associated with Eq. (26) and Eq. (27) are denoted by $\lambda_{j,n'}^{n}$ and $\mu_{j,n}$, respectively. The dual problem of **[P1–A]** is as follows:

[D1]

$$\max \quad \sum_{n'=1}^{n} \overline{\pi}_{j,n'}^{ow} - \sum_{n'=1}^{n} \lambda_{j,n'}^{n} - \mu_{j,n} \Gamma_j^n \tag{28}$$

s.t.

$$\hat{\pi}_{j,n'}^{ow} \le \lambda_{j,n'}^{n} + \mu_{j,n} \quad \forall n' \in [1,n] \tag{29}$$

$$\lambda_{j,n'}^{n} \ge 0 \quad \forall n' \in [1,n] \tag{30}$$

$$\mu_{j,n} \ge 0 \tag{31}$$

For notational convenience, let the feasible domain of [D1] be denoted as U. Accordingly, Eq. (21) is transformed into Eq. (32).

$$\max_{\lambda_{j,n'}^{n}, \mu_{j,n} \in U} \quad \sum_{n'=1}^{n} \overline{\pi}_{j,n'}^{ow} - \sum_{n'=1}^{n} \lambda_{j,n'}^{n} - \mu_{j,n} \Gamma_j^n \ge W_j(n) \quad \forall j \in J, n \in N_j^{cw} \tag{32}$$

To ensure the validity of Eq. (32), it suffices that the constraint holds for any $\lambda_{j,n'}^{n}$ and $\mu_{j,n}$ within U. Thus, Eq. (21) is reformulated as Eqs. (33)–(36).

$$\sum_{n'=1}^{n} \overline{\pi}_{j,n'}^{ow} - \sum_{n'=1}^{n} \lambda_{j,n'}^{n} - \mu_{j,n} \Gamma_j^n \ge W_j(n) \quad \forall j \in J, n \in N_j^{cw} \tag{33}$$

$$\hat{\pi}_{j,n'}^{ow} \le \lambda_{j,n'}^{n} + \mu_{j,n} \quad \forall j \in J, n \in N_j^{cw}, n' \in [1,n] \tag{34}$$

$$\lambda_{j,n'}^{n} \ge 0 \quad \forall j \in J, n \in N_j^{cw}, n' \in [1,n] \tag{35}$$

$$\mu_{j,n} \ge 0 \quad \forall j \in J, n \in N_j^{cw} \tag{36}$$

Next, we derive the constraint ensuring that the SoC at the end of the n-th operating window does not exceed the prescribed upper bound. In Eq. (37), the first term represents the EB's initial battery level at departure, the second term denotes the cumulative amount of energy charged by the end of the $(n-1)$-th charging window, and the third term accounts for the cumulative energy consumption by the same point.

$$b_j^e = \tau_j^{\max}\delta_j + W_j(n-1) - \sum_{n'=1}^{n} \tilde{\pi}_{j,n'}^{ow} \ge \tau_j^{\min}\delta_j \quad \forall j \in J, n \in N_j^{ow}, e = e_{j,n}^{ow} \tag{37}$$

By simplifying Eq. (37), we obtain Eq. (38):

$$\sum_{n'=1}^{n} \tilde{\pi}_{j,n'}^{ow} \le W_j(n-1) + \tau_j^{\max}\delta_j - \tau_j^{\min}\delta_j \quad \forall j \in J, n \in N_j^{ow} \tag{38}$$

The robust counterpart of Eq. (38) is derived following a procedure similar to that of Eq. (21) and is thus omitted. Accordingly, Eq. (38) can be reformulated as Eqs. (39)–(42).

$$\sum_{n'=1}^{n} \bar{\pi}_{j,n'}^{ow} + \sum_{n'=1}^{n} u_{j,n'}^{n} + v_{j,n}\Gamma_j^n \le W_j(n-1) + \tau_j^{\max}\delta_j - \tau_j^{\min}\delta_j \quad \forall j \in J, n \in N_j^{ow} \tag{39}$$

$$\hat{\pi}_{j,n'}^{ow} \le u_{j,n'}^{n} + v_{j,n} \quad \forall j \in J, n \in N_j^{ow}, n' \in [1,n] \tag{40}$$

$$u_{j,n'}^{n} \ge 0 \quad \forall j \in J, n \in N_j^{ow}, n' \in [1,n] \tag{41}$$

$$v_{j,n} \ge 0 \quad \forall j \in J, n \in N_j^{ow} \tag{42}$$

To this end, the robust model is transformed into a tractable mixed integer programming model **[RO-GM]**, which a commercial solver can directly solve. The objective function remains the same as in **[GM]**, while the constraints are modified as follows: Eqs. (1), (5)–(8), (10), (12)–(16), (33)–(36) and (39)–(42).

4. Numerical experiments

This section numerically verifies the proposed R-SC model. It analyzes a real-world case in Lianyungang to discuss the impact of various factors on R-SC planning. The model is coded in Python and Gurobi 11.0.1 with standard tuning implemented on a personal computer with an Intel Core i7-14700KF running at 3.40 GHz and 32 GB RAM.

4.1 Experimental setup

To evaluate the effectiveness of the proposed model, a case study is conducted using actual bus station data from Lianyungang, which is equipped with 10 charging piles. Based on the one-day operational data, the EB operation time chart is shown in Figure 4. A total of 87 EBs operated at this station on that day, serving a total of 286 trips. The planning horizon spans from

5:00 AM to 1:00 AM the following day, based on the earliest and latest operation times of the EBs, with each time slot lasting 10 minutes. In the chart, the blue time slots represent the operating window, corresponding to the periods during which the EBs are in operation. The idle time slots between operating windows are designated as charging windows, representing the periods when the EBs can recharge.

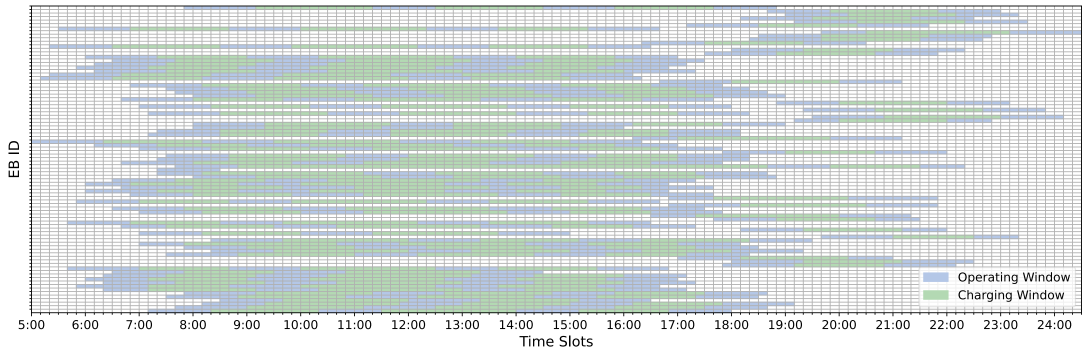

Figure 4 Illustration of EBs' operating windows and charging windows.

The charging requests for private EVs are generated using a stochastic program. The charging duration α_i is randomly selected between 20 and 60 minutes. The total length of the EV charging window is a random value between $[\alpha_i + 20,\ 120]$ in minutes. The start time of the EV charging window is randomly chosen from 8:30 to 18:00.

TOU electricity pricing is considered in this study. The period from 05:00 to 8:00 is defined as off-peak hours, with an electricity price of 0.3193 CNY/kWh. The periods from 8:00 to 11:00 and from 17:00 to 22:00 are defined as peak hours, with an electricity price of 1.1815 CNY/kWh. The periods from 11:00 to 17:00 and from 22:00 to 24:00 are defined as normal hours, with an electricity price of 0.7067 CNY/kWh. Charging piles are set to operate at an efficiency of 150 kW. The total battery capacity of the EBs is specified as 300 kWh, with a minimum charging duration of 20 minutes. To ensure battery health, the maximum SoC is set at 90%, while the minimum SoC is set at 30%. The M2 model parameter Δ is set at 2 hours, which means the soft charging window for EVs is obtained by extending the hard charging window by 2 hours on both ends. The regular price of the service fee $p^{regular}$ is set at 7.5 CNY per time slot. The lower price of the service fee p^{lower} is set at 5 CNY per time slot. The parameter δ controlling the standard deviation of the energy consumption is set to 0.3, and the control parameter Γ_j^n for the uncertainty set is set to 0.1.

4.2 Optimization results and analyses

This section assesses the effectiveness of the R-SC model through numerical experiments. The EB data used is consistent with that provided in Section 4.1, and 500 EV charging requests are generated based on the stochastic program described in Section 4.1.

The results for the four models are presented in Table 2. The row "Total Obj" refers to the overall objective function value of the model. The rows "EB Obj" and "EV Obj" represent the EB charging costs and the net profit from EV charging (i.e., service revenue minus electricity costs), respectively. In terms of computational efficiency, the **[M1]** models outperform the **[M2]** models. This is because the feasible domain of the **[M1]** models is relatively narrower, enabling the branch-and-cut algorithm to converge more quickly. The objective value of the **[M2]** models series model is lower than that of the **[M1]** models, as the **[M2]** models provide more charging opportunities for EVs, thus improving the utilization of available charging resources. The objective values of the robust models are higher than those of their corresponding deterministic models. Although all four models allocate the same total EB charging duration (108 time slots), the robust models incur higher costs because EBs must charge during more expensive time slots to ensure operational reliability.

Table 2 Computational results.

Model	Total Obj	EB Obj	EV Obj	Time (s)
[M1]	−3758.13	**1791.87**	−5550.00	19.60
[M2]	**−4468.13**	**1791.87**	**−6690.00**	70.81
[Robust M1]	−3641.91	1908.09	−5550.00	**12.10**
[Robust M2]	−4351.91	1908.09	**−6690.00**	23.99

In both the **[M1]** and **[M2]** models, the objective function values associated with EB operations are identical, although slight differences exist in the specific charging schedules. Figure 5 depicts the variations in EB energy levels throughout the operational period. During non-operating hours, EBs can undergo centralized charging using low-power chargers, allowing them to begin the following day with a relatively high SoC. While the overall SoC profiles in the **[M1]** and **[M2]** models are largely consistent, the **[M2]** model enhances charging service profitability by adjusting EB charging schedules to accommodate a greater number of EV charging requests. Furthermore, Figure 5 shows that the minimum SoC during EB operations remains around 40%, exceeding the acceptable lower limit of 30%. This is because EBs must retain sufficient energy to complete their subsequent trips, which typically prevents the SoC from approaching the minimum threshold. The maximum SoC during operation reaches the upper limit of 90%, as defined in the model settings.

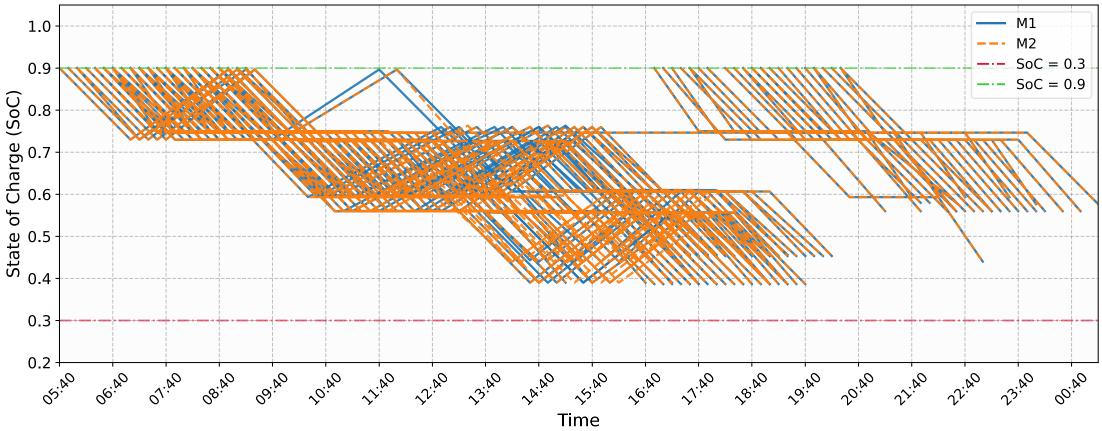

Figure 5 Variations of battery electricity levels of the [M1] model and the [M2] model.

Table 3 summarizes the performance of the four models in terms of EV charging request satisfaction. The row "EV Obj" represents the EV-related component of the objective function, reflecting the profit generated from providing charging services to EVs. The rows "Served EV requests" and "Served EV requests (%)" denote the total number and proportion of EV requests that were successfully served. The row "Total service time (min)" indicates the cumulative duration of all charging services provided to EV requests.

Table 3 EV charging request satisfaction overview.

Model	EV Obj	Served EV requests	Served EV requests (%)	Total service time (min)
[M1]	−5550.00	218.00	43.60	7400.00
[M2]	−6690.00	255.00	51.00	8920.00
[Robust M1]	−5550.00	230.00	46.00	7400.00
[Robust M2]	−6690.00	**258.00**	**51.60**	8920.00

Compared to the **[M1]** models, the **[M2]** models achieve higher charging revenues, serve more EV requests, and provide longer total service durations. These improvements are attributed to the enhanced scheduling flexibility of the **[M2]** models, which offer a broader range of charging options. While the robust models yield the same charging revenues and total service durations as their deterministic counterparts, they exhibit slight differences in the number of served requests. In particular, the robust models tend to favor EV requests with shorter service durations, thereby improving the flexibility of the shared charging strategy.

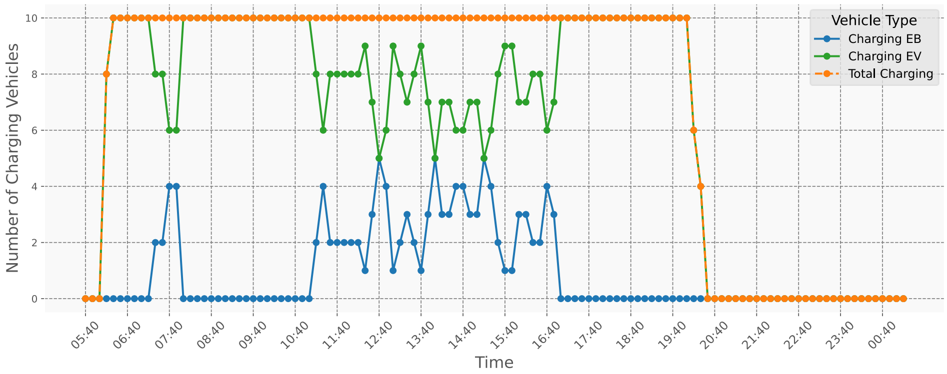

(a) [M1] model

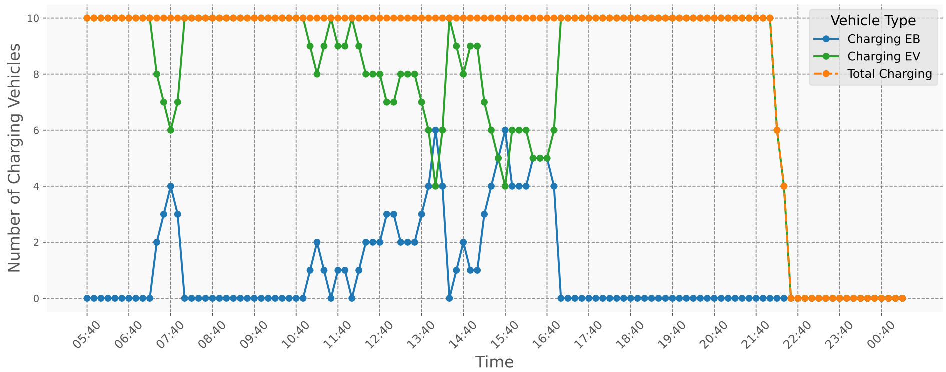

(b) [M2] model

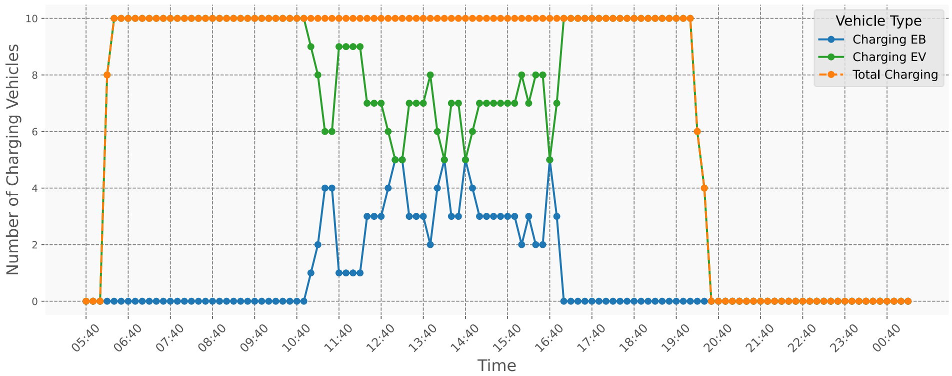

(c) [Robust M1] model

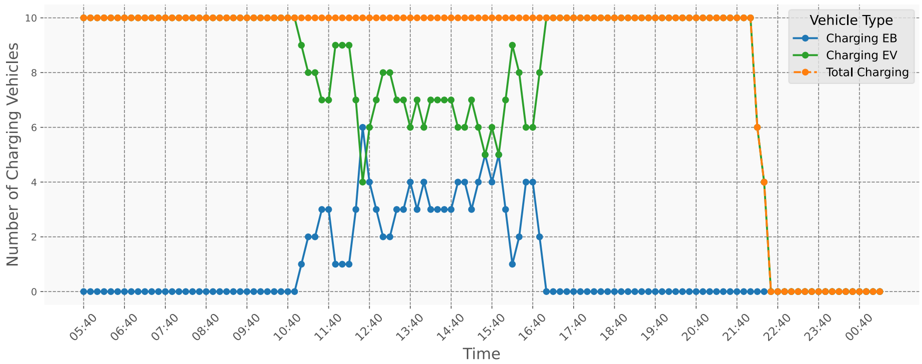

(d) [Robust M2] model

Figure 6 Illustration of charging resource usage over time.

The utilization of charging resources across the four models is shown in Figure 6. In all models, the charging resources are maximally utilized during the period from 6:40 to 20:00. Compared to the **[M1]** model, the **[M2]** model achieves a higher utilization rate of charging resources by extending the available charging time to earlier (5:40–6:40) and later (20:40–22:40) periods for EVs, thereby maximizing the efficiency of the existing charging resources. The robust model, however, delays the charging schedules of some EBs relative to the corresponding deterministic model. While early charging takes advantage of TOU electricity pricing to reduce EB charging costs, it also results in the EB's energy level remaining close to the maximum threshold for extended periods, which may negatively impact the health of the EB's battery.

4.3 Sensitivity analysis

In this section, the impacts of uncertainty parameters and system settings on the R-SC plan are analyzed. The system settings include the number of EV requests, the number of charging piles, the SoC range, and the battery capacity.

4.3.1 Impacts of uncertainty parameters

The parameter δ controls the standard deviation of the energy consumption. As its value increases, the standard deviation of the energy consumption also increases. The parameter of the budgeted uncertainty set is Γ_j^n, and as Γ_j^n increases, the uncertainty in energy consumption grows. The analysis of these uncertain parameters is presented in Table 4. The objective value of the deterministic model is the highest, as the charging strategy for EBs under this model is more conservative, thus allocating additional charging resources to the EVs. As uncertainty increases, the objective value gradually decreases. When $\delta = 1$ and $\Gamma_j^n = 1$, the model becomes infeasible, indicating that the 10 charging piles are insufficient to meet the EB's daytime charging needs under extreme uncertainty.

Table 4 Computational results under different uncertainty parameters.

	Objective value (**[Robust M1]**)	Objective value (**[Robust M2]**)
Deterministic	−3758.13	−4468.13
$\delta = 0.3, \Gamma_j^n = 0.1$	−3641.91	−4351.91
$\delta = 0.7, \Gamma_j^n = 0.8$	−2131.86	−2841.86
$\delta = 1, \Gamma_j^n = 1$	infeasible	infeasible

4.3.2 Impacts of system settings

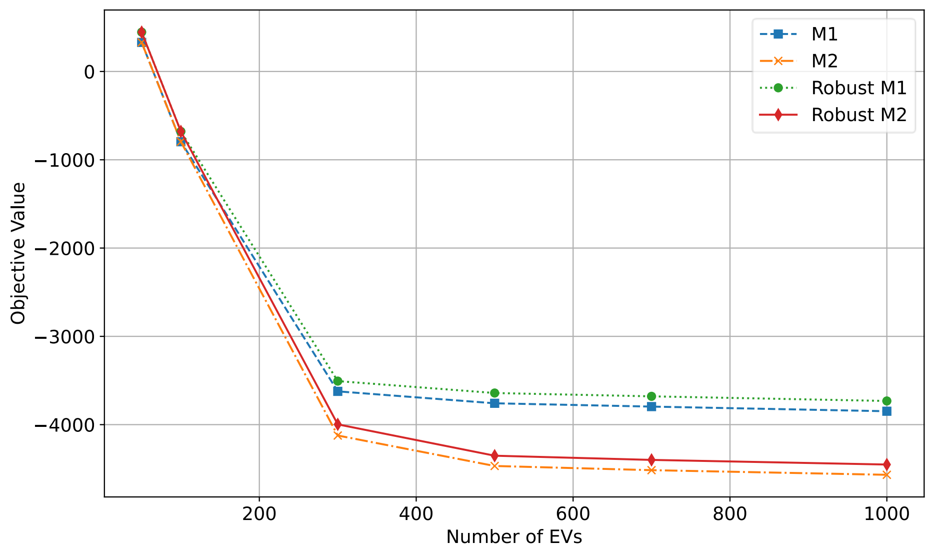

Figure 7 Objective values concerning the number of EVs.

Firstly, the impact of the number of EV requests on the results is analyzed. Keeping other parameters constant, experiments are conducted with the number of EV requests of 50, 100, 300, 500, 700, and 1000. The result is shown in Figure 7. As the number of EV requests increases, the total operational cost for the bus company continually decreases due to the revenue generated from providing charging services to EVs. When the number of EV requests exceeds 100, the objective function becomes negative, indicating that the revenue from opening charging resources exceeds the cost of charging EBs. With fewer EV requests, the difference in the objective function values between the **[M1]** model and the **[M2]** model is small, but this gap widens as the number of EV requests increases. When the number of EV requests exceeds 500, the objective function values stabilize, indicating that this station can accommodate up to approximately 500 EV requests.

Secondly, the impact of the number of charging piles on the results is analyzed. When the number of charging piles is fewer than three, the charging resources are insufficient to support the stable operation of EBs, rendering the model infeasible. Therefore, experiments are conducted with the number of charging piles set at 3, 4, 5, 10, 15, 20, 30, and 50, while keeping other model parameters constant. The experimental results are shown in Figure 8. As the number of charging piles increases, the objective function values steadily decrease and stabilize when the number of charging piles reaches 30. These results suggest that 30 charging piles are sufficient to meet the charging demands of all EBs and EVs at the station, and adding more piles does not yield additional benefits. Additionally, when the number of charging piles is either very limited or abundant, the differences in performance across models become marginal.

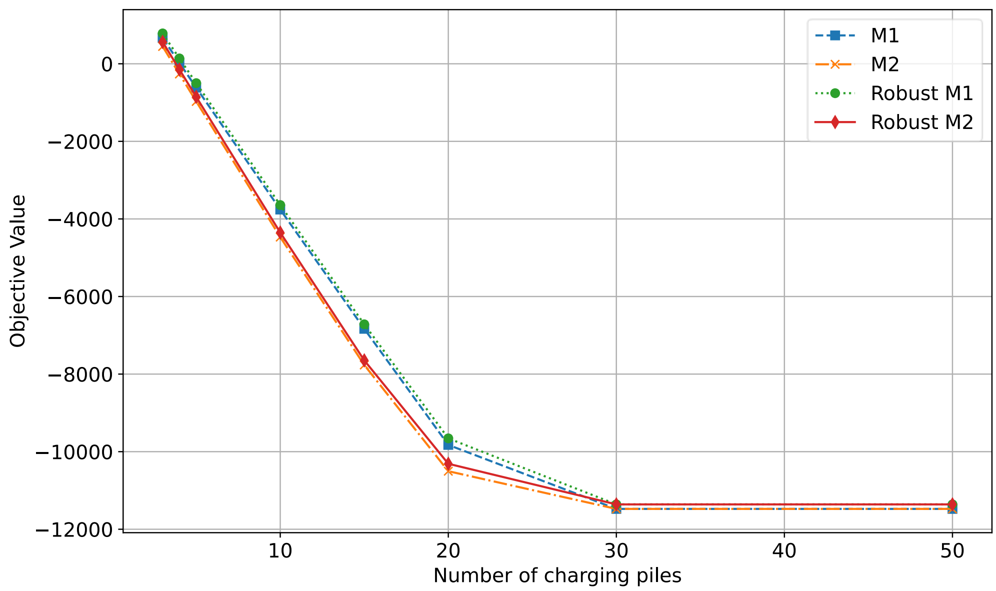

Figure 8 Objective values concerning the number of charging piles.

Thirdly, the impact of the SoC range on the R-SC plan is analyzed. The experimental results are shown in Table 5. When the SoC range is large, EBs do not require charging during the day, resulting in a corresponding objective function value of zero, allowing charging resources to be extensively allocated to EVs. As the SoC range gradually decreases, EBs need to charge more frequently during the day to maintain the SoC within the specified range.

The setting of the SoC range involves a trade-off between battery health and operational costs. A larger SoC range can lead to rapid battery degradation, which is detrimental to long-term operation. Conversely, a smaller SoC range increases the need for frequent charging during the day, thereby reducing the charging resources available for EVs.

Table 5 Objective values concerning the SoC **range.**

SoC Range	Model	Total Obj	EB Obj	EV Obj
$[10\%, 90\%]$	**[M1]**	−6360.00	0.00	−6360.00
	[M2]	−7070.00	0.00	−7500.00
	[Robust M1]	−6360.00	0.00	−6360.00
	[Robust M2]	−7070.00	0.00	−7500.00
$[30\%, 90\%]$	**[M1]**	−3758.13	1791.87	−5550.00
	[M2]	−4468.13	1791.87	−6690.00
	[Robust M1]	−3641.91	1908.09	−5550.00
	[Robust M2]	−4351.91	1908.09	−6690.00
$[40\%, 80\%]$	**[M1]**	−1496.19	3393.82	−4890.00
	[M2]	−2198.69	3393.82	−6015.00
	[Robust M1]	−1379.97	3510.04	−4890.00
	[Robust M2]	−2082.47	3510.04	−6015.00

Fourth, the impact of battery capacity on the results is analyzed (see Figure 9). As the battery capacity increases, the EB can maintain a healthy SoC without charging during the daytime. The release of charging resources allows more EVs to receive charging services, thereby increasing the EB operator's revenue. When the EB's battery capacity reaches 350 kWh, increases in battery capacity do not lead to a further decrease in the objective value. This indicates that a battery capacity of 350 kWh is sufficient to support the current operations at the depot.

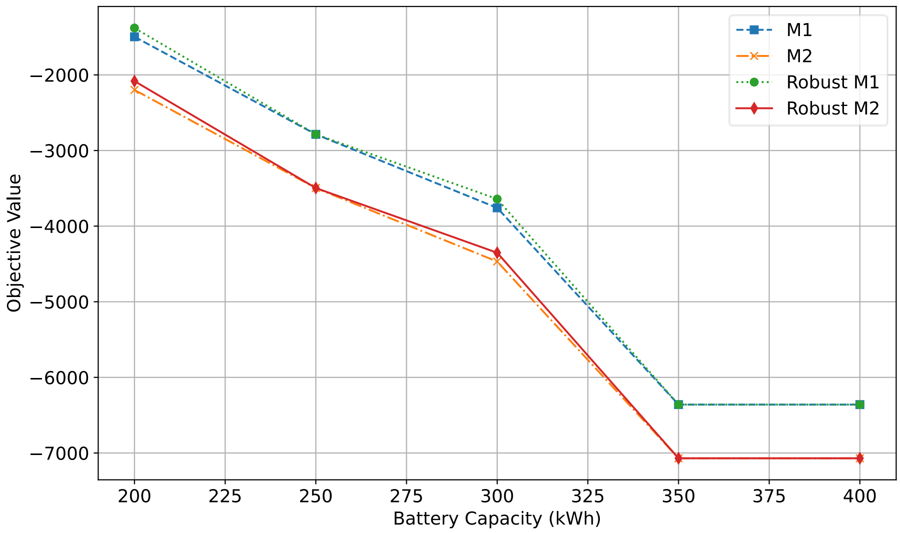

Figure 9 Objective values concerning battery capacity.

Lastly, to evaluate the impact of TOU pricing, the electricity price within the rolling horizon is fixed at 0.7067 CNY/kWh. The results are presented in Table 6. Under low uncertainty levels ($\delta = 0.3, \Gamma_j^n = 0.1$), the robust and deterministic models yield identical outcomes. This is because robust models do not require additional charging but merely shift the timing of charging, which has no cost implication when electricity prices are constant. However, under higher uncertainty ($\delta = 0.7, \Gamma_j^n = 0.8$), robust models result in slightly higher objective values due to increased charging requirements. Overall, the presence of TOU pricing amplifies the impact of uncertainty on SC performance.

Table 6 Computational results without TOU.

Parameters	Model	Total Obj	EB Obj	EV Obj	Time (s)
Deterministic	**[M1]**	−3641.91	1908.09	−5550.00	12.82
	[M2]	−4351.91	1908.09	−6690.00	39.37
$\delta = 0.3, \Gamma_j^n = 0.1$	**[Robust M1]**	−3641.91	1908.09	−5550.00	44.12
	[Robust M2]	−4351.91	1908.09	−6690.00	35.21
$\delta = 0.7, \Gamma_j^n = 0.8$	**[Robust M1]**	−2131.86	2968.14	−5100.00	20.33
	[Robust M2]	−2841.86	2968.14	−6240.00	65.58

5. Conclusions

This study investigates the R-SC problem at a bus depot and develops an integrated optimization model to jointly determine the charging schedules for EBs and EVs. Two distinct pricing strategies are proposed to examine the influence of pricing mechanisms on R-SC planning. Incorporating detailed modeling based on the characteristics of real-world charging scenarios, this study introduces a mixed-integer linear programming model that considers the unique requirements of both EB and EV charging. Moreover, to ensure the stable operation of EBs, a robust model is formulated to account for the uncertainty in the power consumption of EBs. Finally, the robust model is transformed into a tractable formulation using the duality theorem.

Numerical experiments demonstrated the effectiveness of the proposed R-SC model. A real-world case study at Lianyungang Station was conducted, validating the effectiveness of the proposed strategies. The study also analyzed the impact of factors such as the number of EV requests, the number of charging piles, the SoC range, and the battery capacity of EBs on the model results, providing valuable insights for the practical operation of R-SC at bus depots.

In future studies, several potential enhancements could be considered. First, this study focuses on the R-SC problem for a single depot, and the coordinated planning of R-SC across multiple depots within a certain area has yet to be explored. Second, this study assumes all charging piles at the bus depot are homogeneous. Future research could investigate the impact of heterogeneous charging piles on R-SC.

CRediT authorship contribution statement

Di Huang: Conceptualization, Methodology, Writing - Original draft preparation, Writing - Reviewing and Editing. **Zhou Jia**: Conceptualization, Methodology, Software, Writing - Original draft preparation. **Zhitao Hu**: Visualization, Writing - Reviewing and Editing, Validation. **Zhiyuan Liu**: Conceptualization, Writing - Reviewing and Editing, Supervision. **Ronghui Liu**: Conceptualization, Writing - Reviewing and Editing, Supervision.

Declaration of Competing Interest

The authors declare that they have no known competing financial interests or personal relationships that could have appeared to influence the work reported in this paper.

References

[1] Huang D, Wang S. A two-stage stochastic programming model of coordinated electric bus charging scheduling for a hybrid charging scheme. Multimodal Transportation 2022;1:100006. https://doi.org/10.1016/j.multra.2022.100006.

[2] Manzolli JA, Trovão JP, Antunes CH. A review of electric bus vehicles research topics – Methods and trends. Renewable and Sustainable Energy Reviews 2022;159:112211. https://doi.org/10.1016/j.rser.2022.112211.

[3] Niu C, Chen Q, Tu R, Huang D, Ye Y. Co-optimizing electric bus dispatching and charging considering limited resources and battery degradation. Multimodal Transportation 2024;3:100165. https://doi.org/10.1016/j.multra.2024.100165.

[4] Mishra R, Pulugurtha SS, Mathew S. Examining associations with on-time performance and identifying relevant road network, demographic, socioeconomic and land use characteristics within the bus stop vicinity for proactive and reliable public transportation system planning. Multimodal Transportation 2023;2:100094. https://doi.org/10.1016/j.multra.2023.100094.

[5] Najafi A, Gao K, Parishwad O, Pourakbari-Kasmaei M, Precup R-E, Roman R-C. Integrated planning, operation and optimization of coupled transportation and energy systems. Multimodal Transportation 2025;4:100199. https://doi.org/10.1016/j.multra.2025.100199.

[6] Rogge M, Van Der Hurk E, Larsen A, Sauer DU. Electric bus fleet size and mix problem with optimization of charging infrastructure. Applied Energy 2018;211:282–95. https://doi.org/10.1016/j.apenergy.2017.11.051.

[7] Kim J, Son S-Y, Lee J-M, Ha H-T. Scheduling and performance analysis under a stochastic model for electric vehicle charging stations. Omega 2017;66:278–89. https://doi.org/10.1016/j.omega.2015.11.010.

[8] Sun H, Yang J, Yang C. A robust optimization approach to multi-interval location-inventory and recharging planning for electric vehicles. Omega 2019;86:59–75. https://doi.org/10.1016/j.omega.2018.06.013.

[9] Zeng X, Xie C. A comparative analysis of modeling and solution methods for the en-route charging station location problems within uncongested and congested highway networks. Multimodal Transportation 2024;3:100150. https://doi.org/10.1016/j.multra.2024.100150.

[10] Gong D, Tang M, Buchmeister B, Zhang H. Solving location problem for electric vehicle charging stations—A sharing charging model. IEEE Access 2019;7:138391–402. https://doi.org/10.1109/ACCESS.2019.2943079.

[11] Zaidi I, Oulamara A, Idoumghar L, Basset M. Maximizing the number of satisfied charging demands of electric vehicles on identical chargers. Omega 2024;127:103106. https://doi.org/10.1016/j.omega.2024.103106.

[12] Huawei. Huawei's ultra-fast charging technology activates the resource endowment of public transportation, supporting the transformation and upgrading of bus companies towards new energy solutions 2024. Available at: https://digitalpower.huawei.com/cn/smartchargingnetwork/news/detail/2372.html.

[13] Ye Z, Yu N, Wei R, Liu XC. Decarbonizing regional multi-model transportation system with shared electric charging hubs. Transportation Research Part C: Emerging Technologies 2022;144:103881. https://doi.org/10.1016/j.trc.2022.103881.

[14] Zhang M, Yang M, Gao Y. Tripartite evolutionary game and simulation analysis of electric bus charging facility sharing under the governmental reward and punishment mechanism. Energy 2024;307:132783. https://doi.org/10.1016/j.energy.2024.132783.

[15] Ji J, Bie Y, Wang L. Optimal electric bus fleet scheduling for a route with charging facility sharing. Transportation Research Part C: Emerging Technologies 2023;147:104010. https://doi.org/10.1016/j.trc.2022.104010.

[16] Liu Z, Ma X, Zhuo S, Liu X. Optimizing shared charging services at sustainable bus charging hubs: A queue theory integration approach. Renewable Energy 2024;237:121860. https://doi.org/10.1016/j.renene.2024.121860.

[17] Perumal SSG, Lusby RM, Larsen J. Electric bus planning & scheduling: A review of related problems and methodologies. European Journal of Operational Research 2022;301:395–413. https://doi.org/10.1016/j.ejor.2021.10.058.

[18] Abdelwahed A, Van Den Berg PL, Brandt T, Collins J, Ketter W. Evaluating and optimizing opportunity fast-charging schedules in transit battery electric bus networks. Transportation Science 2020;54:1601–15. https://doi.org/10.1287/trsc.2020.0982.

[19] Liu K, Gao H, Liang Z, Zhao M, Li C. Optimal charging strategy for large-scale electric buses considering resource constraints. Transportation Research Part D: Transport and Environment 2021;99:103009. https://doi.org/10.1016/j.trd.2021.103009.

[20] Whitaker J, Droge G, Hansen M, Mortensen D, Gunther J. A network flow approach to battery electric bus scheduling. IEEE Trans Intell Transport Syst 2023;24:9098–109. https://doi.org/10.1109/TITS.2023.3276269.

[21] Zeng Z, Wang S, Qu X. On the role of battery degradation in en-route charge scheduling for an electric bus system. Transportation Research Part E: Logistics and Transportation Review 2022;161:102727. https://doi.org/10.1016/j.tre.2022.102727.

[22] Bao Z, Li J, Bai X, Xie C, Chen Z, Xu M, et al. An optimal charging scheduling model and algorithm for electric buses. Applied Energy 2023;332:120512. https://doi.org/10.1016/j.apenergy.2022.120512.

[23] Wu W, Lin Y, Liu R, Jin W. The multi-depot electric vehicle scheduling problem with power grid characteristics. Transportation Research Part B: Methodological 2022;155:322–47. https://doi.org/10.1016/j.trb.2021.11.007.

[24] Wu W, Lin Y, Liu R, Li Y, Zhang Y, Ma C. Online EV charge scheduling based on time-of-use pricing and peak load minimization: Properties and efficient algorithms. IEEE Trans Intell Transport Syst 2022;23:572–86. https://doi.org/10.1109/tits.2020.3014088.

[25] Yang S, An K, Rich J. Electric bus battery swapping and charging management across multiple depots. Omega 2026;138:103434. https://doi.org/10.1016/j.omega.2025.103434.

[26] An K. Battery electric bus infrastructure planning under demand uncertainty. Transportation Research Part C: Emerging Technologies 2020;111:572–87. https://doi.org/10.1016/j.trc.2020.01.009.

[27] Zeng Z, Wang T, Qu X. En-route charge scheduling for an electric bus network: Stochasticity and real-world practice. Transportation Research Part E: Logistics and Transportation Review 2024;185:103498. https://doi.org/10.1016/j.tre.2024.103498.
[28] Zhou Y, Wang H, Wang Y, Li R. Robust optimization for integrated planning of electric-bus charger deployment and charging scheduling. Transportation Research Part D: Transport and Environment 2022;110:103410. https://doi.org/10.1016/j.trd.2022.103410.
[29] Huang D, Zhang J, Liu Z. A robust coordinated charging scheduling approach for hybrid electric bus charging systems. Transportation Research Part D: Transport and Environment 2023;125:103955. https://doi.org/10.1016/j.trd.2023.103955.
[30] Wang G, Li W, Zhang J, Ge Y, Fu Z, Zhang F, et al. sharedCharging: Data-driven shared charging for large-scale heterogeneous electric vehicle fleets. Proc ACM Interact Mob Wearable Ubiquitous Technol 2019;3:1–25. https://doi.org/10.1145/3351266.
[31] Jia Z, An K, Ma W. Utilizing electric bus depots for public Charging: Operation strategies and benefit analysis. Transportation Research Part D: Transport and Environment 2024;130:104155. https://doi.org/10.1016/j.trd.2024.104155.
[32] Bertsimas D, Sim M. The price of robustness. Operations Research 2004;52:35–53. https://doi.org/10.1287/opre.1030.0065.
[33] Govindan K, Fattahi M, Keyvanshokooh E. Supply chain network design under uncertainty: A comprehensive review and future research directions. European Journal of Operational Research 2017;263:108–41. https://doi.org/10.1016/j.ejor.2017.04.009.
[34] Roald LA, Pozo D, Papavasiliou A, Molzahn DK, Kazempour J, Conejo A. Power systems optimization under uncertainty: A review of methods and applications. Electric Power Systems Research 2023;214:108725. https://doi.org/10.1016/j.epsr.2022.108725.
[35] Rodrigues F, Agra A. Berth allocation and quay crane assignment/scheduling problem under uncertainty: A survey. European Journal of Operational Research 2022;303:501–24. https://doi.org/10.1016/j.ejor.2021.12.040.
[36] Gorissen BL, Yanıkoğlu İ, Den Hertog D. A practical guide to robust optimization. Omega 2015;53:124–37. https://doi.org/10.1016/j.omega.2014.12.006.